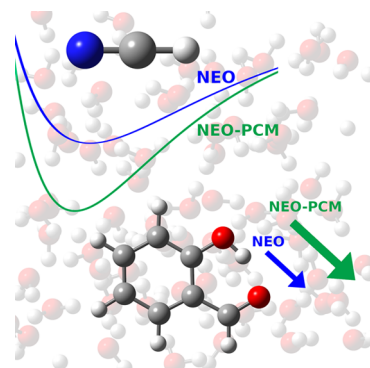


Solvated Nuclear–Electronic Orbital Structure and Dynamics

Andrew Wildman, Zhen Tao, Luning Zhao, Sharon Hammes-Schiffer,* and Xiaosong Li*

ABSTRACT: Nonadiabatic dynamical processes such as proton-coupled electron transfer and excited state intramolecular proton transfer have been the subject of much research. One of the promising theoretical methods to describe these processes is the nuclear–electronic orbital (NEO) approach. This approach inherently accounts for nuclear quantum effects within quantum chemistry calculations, and it has recently been extended to directly simulate nonadiabatic processes with the development of real-time NEO methods. These processes can also be significantly dependent on the surrounding chemical environment, however, and capturing the effects of the environment is often necessary for analyzing experimentally relevant systems. This work couples the NEO density functional theory and real-time time-dependent density functional theory approaches with solvation through the polarizable continuum model. The effects of this coupling are investigated for ground state properties, solvent-dependent vibrational frequencies, and direct excited state intramolecular proton transfer dynamics.



INTRODUCTION

Nonadiabatic dynamical processes such as proton-coupled electron transfer (PCET) and excited state intramolecular proton transfer (ESIPT) require careful treatment of the coupled nuclear and electronic quantum subsystems. At the same time, experimental studies of these processes are often performed in solution, and the solvation environment can strongly affect the dynamics of these processes.¹

Of the many approaches used to account for coupled quantum nuclear and electronic structure,^{2–15} the nuclear–electronic orbital (NEO) approach provides a particularly efficient method for treating electrons and select protons quantum mechanically on the same footing.^{16–20} The NEO approach naturally incorporates nuclear quantum effects, such as zero-point energy (ZPE) and quantized vibrational states. Furthermore, the NEO approach has recently been extended to allow for direct coupled time propagation of the quantum electrons and protons.^{18,21} This real-time NEO (RT-NEO) approach has shown particular promise in the direct simulation of nonadiabatic processes such as PCET and ESIPT.²²

In order for these newly developed approaches to be applicable to understanding experiments, the effects of solvation and the chemical environment must also be taken into account. One of the most widely used methods to account for solvent effects is the polarizable continuum model (PCM).^{23–26} In the most common form of this model, the quantum mechanical molecule is placed within a uniform dielectric with the permittivity of the solvent, and the effects of solvation are captured through the polarization of this dielectric.^{24,26} The PCM approach has been thoroughly studied, in both the time-independent²⁷ and time-dependent^{28–31} domains, and it has been shown to be a robust model

for capturing solvent effects on the ground state and within dynamical processes.²⁶

However, the effects of solvation within the NEO framework are yet unknown. In this work, the NEO Hartree–Fock (NEO-HF) and NEO density functional theory (NEO-DFT) methods, as well as their time-dependent counterparts, are coupled with PCM, and the resulting phenomena are investigated. First, the theory required to couple these two formalisms is presented. Next, the effects of solvation on the ground state properties of NEO-DFT wave functions are analyzed through a case study of hydrogen cyanide (HCN) in many different solvents. Solvation in time-dependent properties is then captured through the use of the RT-NEO formalism, and the resulting solvation effects on the electronic and vibrational spectra of HCN are investigated. Finally, direct simulation of ESIPT in a vacuum and in solvent is performed, demonstrating the significant effects solvation can have on these processes.

THEORY

Both the theory of the NEO method^{18,20} and the theory of PCM^{24,26} are well described elsewhere. Here, we briefly review the equations necessary to couple these two approaches with an emphasis on the time-dependent formulation. For time-

independent processes such as wave function optimization, the following equations reduce to time-independent forms trivially.

The time-dependent NEO formalism for single-determinant methods takes the following product ansatz:

$$\Psi_{\text{NEO}}(t) = \Phi_e(t) \Phi_p(t) \quad (1)$$

where Φ_e and Φ_p are Slater determinants for the electrons and protons, respectively. This ansatz leads to two coupled Von Neumann equations that determine the dynamics of the protons and the electrons:

$$\begin{aligned} i \frac{\partial}{\partial t} \mathbf{P}^e(t) &= [\mathbf{F}^e(t, \mathbf{P}^e(t), \mathbf{P}^p(t)), \mathbf{P}^e(t)] \\ i \frac{\partial}{\partial t} \mathbf{P}^p(t) &= [\mathbf{F}^p(t, \mathbf{P}^p(t), \mathbf{P}^e(t)), \mathbf{P}^p(t)] \end{aligned} \quad (2)$$

where $\mathbf{P}^x(t)$ is the time-dependent density matrix for the electrons ($x = e$) or protons ($x = p$) and $\mathbf{F}^x(t)$ is the time-dependent Fock matrix for each subsystem in an orthonormal basis.

In order to couple a NEO wave function with a polarizable medium, one needs to account for the mutual polarization between the NEO quantum system and the classically polarizable system. This interaction is accounted for by introducing a solvent operator, $\mathbf{V}^{\text{PCM}}(\mathbf{P}^e(t), \mathbf{P}^p(t))$, that is dependent on both the electronic and protonic time-dependent densities. This operator is directly added into the Fock matrices of both the electrons and the protons:

$$\begin{aligned} \mathbf{F}^e(t) &= \mathbf{F}^{e,0}(t, \mathbf{P}^e(t), \mathbf{P}^p(t)) - \mathbf{V}^{\text{PCM}}(\mathbf{P}^e(t), \mathbf{P}^p(t)) \\ \mathbf{F}^p(t) &= \mathbf{F}^{p,0}(t, \mathbf{P}^p(t), \mathbf{P}^e(t)) + \mathbf{V}^{\text{PCM}}(\mathbf{P}^e(t), \mathbf{P}^p(t)) \end{aligned} \quad (3)$$

where $\mathbf{F}^{x,0}$ is the Fock matrix for either the electronic or protonic component in a vacuum. The difference in sign originates from the opposite charge of electrons and protons. Taking the most common approach to solving the PCM equations, a boundary surface surrounding the molecule is defined and discretized into tesserae with apparent charges, q_i , and centers \mathcal{R}_i . The solvent operator expressed over the basis set for each subsystem (μ, ν, \dots) has an identical form, given by

$$V_{\mu,\nu}^{\text{PCM}} = \sum_i \langle \mu | \frac{q_i(\mathbf{P}^e(t), \mathbf{P}^p(t))}{|\mathbf{r} - \mathcal{R}_i|} | \nu \rangle \quad (4)$$

Solving for the apparent surface charge at each tessera, q_i , depends on the exact PCM formalism used. The differences and solutions for these various formalisms are given in detail elsewhere,²³ but the common elements among all formalisms is that the charge at each tessera depends both on the total charge density (electron, proton, and classical nuclei) in the quantum mechanical region and on the charges of all other tesserae. Furthermore, the polarization of the cavity relies on the frequency-dependent dielectric function, $\epsilon(\omega)$, of the solvent used. Directly accounting for this frequency dependence is possible,^{30,31} but it can be computationally expensive for long simulations and can be avoided when the absorption bands of the solvent and solute do not overlap significantly.

Another approach is to partition the surface charge into “fast” and “slow” components: these correspond to the high-frequency electronic response and low-frequency orientational and vibrational response, respectively.²⁴

$$q_i = q_i^{\text{slow}} + q_i^{\text{fast}} \quad (5)$$

For time-independent problems, such as optimization of the ground state NEO wave function, both the fast and slow components are allowed to respond and optimize, and the total surface charge is determined by the static permittivity of the solvent, ϵ_0 . For time-dependent problems, such as real-time propagation of a NEO wave function, the fast component is allowed to respond instantaneously to the changes in electron and proton density with the high-frequency permittivity of the solvent, ϵ_∞ , but the slow component is kept static for the duration of the simulation. When using this approach, the time dependence of the polarization of the cavity is solely through the fast component response to the time-dependent density,^{29,32} not through an explicit equation of motion for the polarization of the cavity.^{33–37}

■ GROUND STATE PCM-NEO

The time-independent PCM-NEO-DFT formalism is used to study the ground state properties of the HCN molecule in a variety of solvents. HCN has been studied extensively as a benchmark for NEO methods, and it is a well-suited molecule for studying solvation because it has a strong dipole moment that may be accentuated by solvation. To investigate the interaction between solvation provided through PCM and the NEO-DFT wave function, the ground state properties of HCN were calculated both using a classical proton and using the NEO approach. For each approach, the HCN molecule was placed in a vacuum and PCM solvent corresponding to the static permittivities of cyclohexane, tetrahydrofuran, acetonitrile, acetone, and water. In all cases, the same geometry and basis function centers were used.

All calculations were performed with the ChronusQuantum open source electronic structure package.^{38,39} The cc-pVDZ electronic basis set⁴⁰ was used for the electronic subsystem, and the PB4-F2 protonic basis set⁴¹ was used for the proton. Electron correlation and exchange was treated with the B3LYP functional,^{42–45} and electron–proton correlation was treated with the epc17-2 functional.^{17,46} The HCN geometry was obtained from a geometry optimization at the NEO-DFT level with the same functionals and electronic basis set as specified above and a protonic 8s8p8d even-tempered basis set.¹⁷ For the conventional DFT calculations, the proton was placed at the location of the NEO-optimized protonic basis function centers. The PCM equations were solved by using the PCMSolver package⁴⁷ using the isotropic IEF-PCM formalism. The cavity was generated for the solvent excluding surface (SES) by considering spheres with radii 1.2 times the Bondi van der Waals radii⁴⁸ on all classical atoms and protonic basis function centers. For the purposes of cavity generation, protonic basis function centers were considered to be hydrogens.

When placed in a solvent, the total energy of the whole system decreases for both the classical and NEO approaches, and the amount of stabilization of the system increases with increasing permittivity, as seen in Figure 1. Interestingly, the ZPE, here defined as the difference between the classical and NEO energies, increases as a function of permittivity as well.

Additionally, one can compare the change in molecular dipole moment as a function of solvent permittivity. In classical PCM electronic structure calculations, the total molecular dipole moment is expected to increase with solvent permittivity for polar molecules because the cavity stabilizes greater separation of charges within the quantum molecule through the surface charge.²⁴ As expected, this trend is

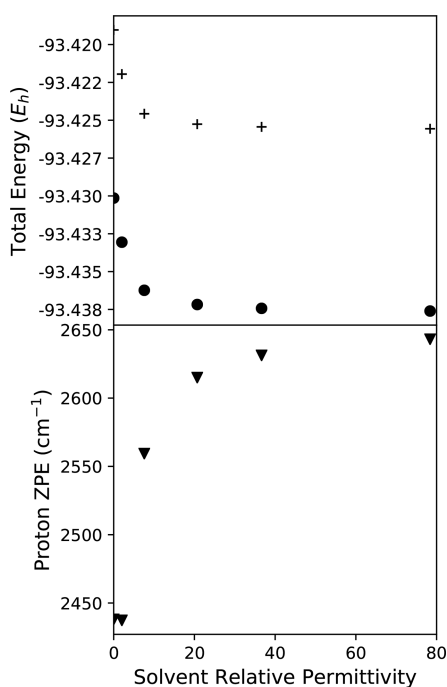


Figure 1. Energetics of HCN in a variety of solvents with a classical proton description (circles) and with a NEO protonic wave function (crosses). The protonic zero-point energy is shown with triangles.

observed for the HCN system with a classical proton, shown in Figure 2. However, a surprising result is observed for the HCN system by using NEO-DFT: almost no change in molecular dipole moment is observed as a function of solvent permittivity. This behavior can be explained by examining the C–H distance in the various solvents, measured as the

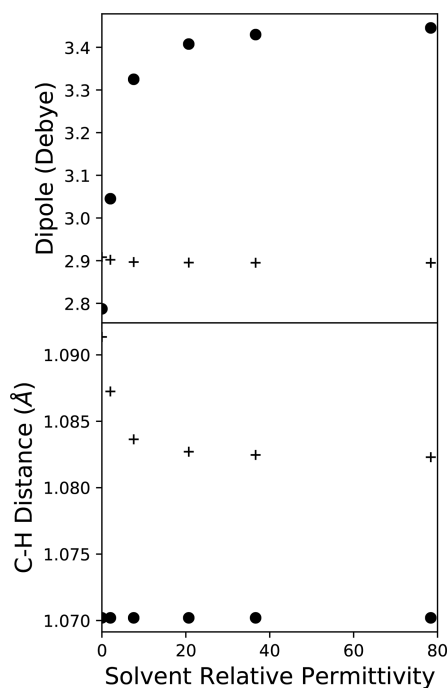


Figure 2. Total molecular dipole moment (top) and C–H bond length (bottom) of HCN in a variety of solvents with a classical description (circles) and with a NEO protonic wave function (crosses).

distance between the position of the classical carbon nucleus and the expectation value of the proton position. While the position of the classical proton is fixed and the basis function center is fixed for the quantum proton, the expectation value of the quantum proton position can shift in response to the various solvation environments due to the higher angular momentum basis functions. As shown in Figure 2, the NEO C–H distance decreases with increasing solvent permittivity. This change in C–H bond length in the different solvent environments counteracts the expected increase in dipole moment, leading to an effectively stationary molecular dipole moment.

Both the decrease in C–H bond length and the increase in ZPE can be explained by considering the effect of a molecular cavity with a surface charge surrounding the quantum proton. In a molecule with a terminal proton, such as HCN, the potential acting on that proton is asymmetric—repulsion steeply increases as the proton moves from the equilibrium bonding position toward the carbon, but only gradually increases as it moves away from the carbon along the C–H dissociation coordinate. When a solvent environment is introduced around the molecule, the potential along the C–H dissociation coordinate is expected to increase, leading to a steeper potential wall. This steeper wall would cause the expectation value of the proton position to move toward the carbon, shortening the C–H bond and increasing the ZPE.

■ VIBRATIONAL SOLVATOCHROMIC SHIFTS

The formate ion, CO_2H^- , depicted in Figure 3, exhibits vibrational solvatochromism,⁴⁹ making it an ideal candidate to

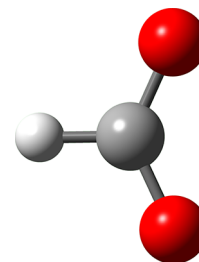


Figure 3. Structure of the formate ion, CO_2H^- .

investigate the effects of solvent on excited states within the NEO framework. In this section, we will use real-time dynamics to extract the linear absorption spectra from the formate ion in both vacuum and water. The real-time NEO approach has been shown to be an effective method to generate linear absorption spectra¹⁸ without requiring formation of the orbital Hessian.

The formate ion was modeled with the NEO approach using the PB4-F2 protonic basis set and a split electronic basis set: cc-pVTZ⁵⁰ on the carbon and oxygen atoms and a modified cc-pV6Z⁵¹ on the protonic center, where the $L = 5$ angular momentum basis functions have been removed. The geometry was obtained by a conventional electronic Hartree–Fock geometry optimization with the previously described split cc-pVTZ/cc-pV6Z electronic basis set. The electronic and protonic basis function centers for the hydrogen were placed at the position of the classical hydrogen in the optimized geometry. The SES was generated in the same manner as for HCN, and only the surface charge, not the SES geometry, was allowed to change during the simulation. The vibrational

spectrum was extracted from the Fourier transform of the dipole impulse response from three orthogonal directions.^{18,21} These simulations were carried out both in a vacuum and in PCM water in order to capture the solvatochromism.

These results are compared to anharmonic calculations using second-order vibrational perturbation theory⁵² (VPT2) on a conventional electronic structure calculation. The same split electronic basis set was used, and the masses of the carbon and oxygen atoms were set to artificially high values in order to isolate the proton vibrational response and provide equivalent vibrations to the proton-only vibrations that arise from RT-NEO calculations. All VPT2 vibrational calculations were performed with the Gaussian computational chemistry software package.⁵³

A final reference point is given by the experimental values for the C–H vibration in a neutral Ne lattice⁵⁴ and in water.⁵⁵ Because our theoretical calculations do not include carbon and oxygen motion in the vibrational modes, the absolute frequencies are not expected to agree; performing VPT2 on the whole molecule at the same level of theory without artificially high masses provides a stretch frequency of 2474 cm^{-1} , demonstrating that the artificial masses are the primary source of discrepancy in absolute frequencies. Instead, the experimental values are included to provide a reference point for the expected solvatochromic shift.

The CH vibrational frequencies and spectroscopic shifts from a neutral environment to water for all systems are found in Table 1. In all systems, the introduction of solvent increases

Table 1. C–H Vibrational Frequencies of the Formate Ion Obtained with a Variety of Models in a Neutral Environment and Water

proton model	environment	excitation frequency (cm^{-1})	solvatochromic shift (cm^{-1})
conventional VPT2	vacuum	2570	–
conventional VPT2	water	2711	141
RT-NEO-HF	vacuum	2699	–
RT-NEO-HF	water	2813	114
experimental ⁵⁴	Ne lattice	2456	–
experimental ⁵⁵	water	2803	347

the vibrational frequency, demonstrating that the polarizable medium introduces some of the correct solvent–solute interaction. However, by inspecting the solvatochromic shifts directly, we see that the total shift in the computational models is less than half that of the experimental shift, showing that some essential physics of this solvatochromic shift is not being captured. In particular, harmonic frequencies in a vacuum and in solution with and without artificially high masses show solvatochromic shifts of 119 and 320 cm^{-1} , respectively, suggesting that a large portion of the solvatochromic shift that is not captured are the vibrational contributions from the nonprotonic nuclei. Moreover, isolating the proton vibrations from the other nuclear motions, which are expected to be coupled to some extent, impacts the effect of the solvent on all of the molecular vibrational frequencies. There may also be error that arises from the solvent model; treating solvent interactions with PCM necessarily neglects specific solute–solvent interactions, such as hydrogen bonding, which contributes to solvatochromism.⁵⁶ Accurate treatment of these aspects requires treating solvent molecules explicitly

with a model such as polarizable molecular mechanics⁵⁷ and moving beyond the PCM embedded RT-NEO model, e.g., obtaining vibrational frequencies of the entire molecule from NEO-Ehrenfest dynamics⁵⁸ or NEO-DFT(V).⁵⁹

■ SOLVATED PROTON TRANSFER DYNAMICS

The real-time NEO approach has been demonstrated to be effective for simulating ESIPT,¹⁸ and this process can be modulated by the solvation environment of the molecule undergoing ESIPT.⁶⁰ Here, we present the ESIPT of *o*-hydroxybenzaldehyde (*o*HBA) simulated by RT-NEO-TDDFT in both a vacuum and water. Because the ESIPT of *o*HBA has been studied by both experimental techniques and RT-NEO-TDDFT previously, it serves as a good gauge of the ability of PCM to capture the solvent modulation of proton transfer processes described by the NEO approach.

In order to capture the ESIPT without motion of the heavy nuclei, one must begin from an excited state geometry.¹⁸ The geometry used for this simulation was the restricted excited state geometry obtained from Aquino et al.⁶¹ by optimizing the geometry on the excited surface with the oxygen donor–hydrogen distance constrained to its ground state value. The cc-pVDZ basis set was used for the electrons, and a minimal, even-tempered sp basis set with exponents of 4.0 was used for the proton. The initial electronic and protonic basis function centers for the transferring hydrogen were placed at the position of the classical hydrogen in the restricted excited state geometry. To provide enough flexibility along the proton transfer coordinate to capture the ESIPT, additional basis function centers were added along the proton transfer path, as shown in Figure 4. The SES was generated in the same manner

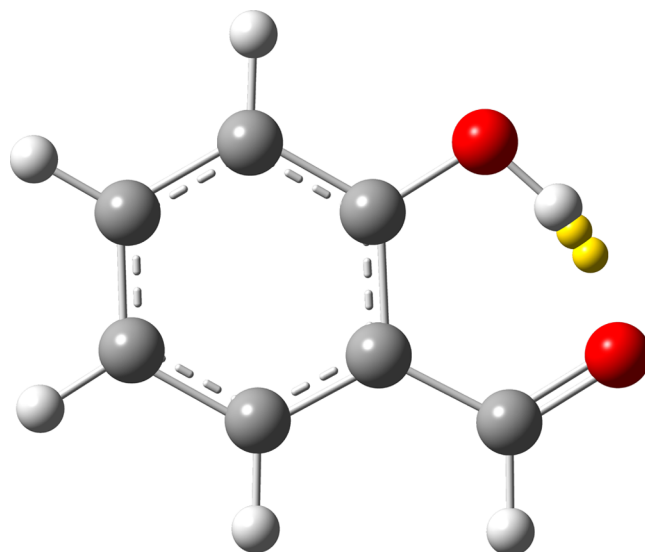


Figure 4. Restricted excited state structure of *o*HBA. The additional basis function centers are marked with yellow spheres.

as for HCN, and only the surface charge, not the SES geometry, was allowed to change during the simulation. Note that this creates an unbiased SES across the proton transfer coordinate, although the change to the surface caused by the additional protonic basis function centers is small (see the Supporting Information for details). The B3LYP functional was used for electron correlation and exchange, and the epc17-2 functional was used for electron–proton correlation. The

initial state was prepared by a HOMO–LUMO swap prior to propagation.

The distances between the expectation values of the quantum proton position and the donor and acceptor oxygens are shown in Figure 5 for simulations both in a vacuum and in

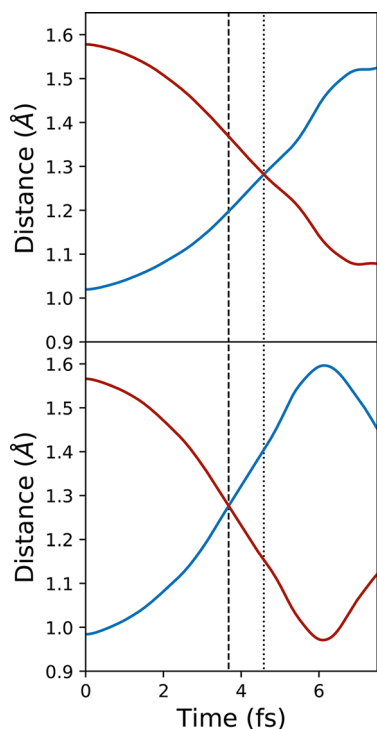


Figure 5. Excited state intramolecular proton transfer in oHBA in a vacuum (top) and in water (bottom) for the restricted excited state geometry. The distance between the expectation value of the transferring proton position and the donor oxygen (blue) and acceptor oxygen (red) is given as a function of time. The crossing time in a vacuum is marked with the vertical dotted line, and the crossing time in water is marked with the vertical dashed line.

water. The proton transfer time can be defined as the time at which these two distances are identical. The proton transfers to the acceptor oxygen approximately 4.6 fs after excitation in a vacuum but after only approximately 3.7 fs in water. These extremely fast proton transfer times arise because all nuclei except the transferring proton are fixed to their coordinates in the excited state geometry. The acceleration in water is primarily due to differences in the ground state solvation; when the “fast” response of the solvent is neglected entirely and propagation is only within the static field of the ground state PCM, the acceleration is still observed. It is likely that the difference in initial proton position in a vacuum and in water is responsible for the acceleration, as the HOMO–LUMO swap prepares a $\pi\pi^*$ antibonding state between the donor oxygen and proton. This acceleration is still observed when the dynamics are performed without PCM but with the initial wave function determined in the presence of PCM, further supporting the implication that this effect is due to solvent-driven differences in the ground state (details in the Supporting Information). With the shorter O–H bond obtained from the expectation value of the proton position in the solvated NEO-DFT ground state, the initial repulsion is greater upon the HOMO–LUMO swap, driving the transfer to occur faster.

It is worth noting that using the nonequilibrium approach during processes that involve nuclear motion neglects polarization in the solvent due to nuclear movement, which may be on the same time scale as the simulation. Other approaches can propagate the polarization of the cavity according to an equation of motion,^{30,31} and these may give more accurate results for processes that involve solute nuclear motion. In the work presented here, however, the acceleration of proton transfer is observed even in the limit that all polarization of the solvent environment is able to come to equilibrium with the changes in the solute (see the Supporting Information for details).

CONCLUSION

In this work, the NEO approach was coupled with the PCM solvation model. The effects of this solvation were investigated on both ground state and time-dependent excited state properties. In both cases, solvation is shown to have a significant effect. Furthermore, the use of a NEO description of protons introduces novel effects of solvation compared to solvation of molecules with classical protons. Specifically, classically expected trends of increasing dipole moment and solvatochromism are influenced by the quantum nature of the proton, and explanations of the effects of solvation must take these issues directly into account.

The approach to model solvation used in this work relies on a continuum description of the solvent. This method offers some significant advantages, such as implicit integration over all solvent degrees of freedom, but it also cannot model all processes important for solvation. In particular, hydrogen bonding between the solute and the solvent can be important for many processes, and this importance is only expected to increase for systems in which protons are described quantum mechanically. Further work will extend the polarizable coupling between NEO wave functions and their environments to solvent descriptions with explicit nuclear degrees of freedom, such as polarizable molecular mechanics. For solvents without hydrogen bonding to the solute, the current approach shows promise for modeling coupled nuclear–electronic wave functions within a responsive solvent environment. Additional work will extend the equilibrium time-dependent solvation model used here to a direct equation of motion for the solvent.

ASSOCIATED CONTENT

Supporting Information

The Supporting Information is available free of charge at <https://pubs.acs.org/doi/10.1021/acs.jctc.1c01285>.

Computational details; additional simulations (PDF)

AUTHOR INFORMATION

Corresponding Authors

Sharon Hammes-Schiffer – Department of Chemistry, Yale University, New Haven, Connecticut 06520, United States; orcid.org/0000-0002-3782-6995;

Email: sharon.hammes-schiffer@yale.edu

Xiaosong Li – Department of Chemistry, University of Washington, Seattle, Washington 98195, United States; Pacific Northwest National Laboratory, Richland, Washington 99354, United States; orcid.org/0000-0001-7341-6240; Email: xsli@uw.edu

Authors

Andrew Wildman – Department of Chemistry, University of Washington, Seattle, Washington 98195, United States;

orcid.org/0000-0001-7013-6550

Zhen Tao – Department of Chemistry, Yale University, New Haven, Connecticut 06520, United States; orcid.org/0000-0003-0511-7665

Luning Zhao – Department of Chemistry, University of Washington, Seattle, Washington 98195, United States;

orcid.org/0000-0002-8989-3751

Complete contact information is available at:

<https://pubs.acs.org/10.1021/acs.jctc.1c01285>

Notes

The authors declare no competing financial interest.

ACKNOWLEDGMENTS

The development of quantum dynamics for studies of proton transfer was supported by IDREAM (Interfacial Dynamics in Radioactive Environments and Materials), an Energy Frontier Research Center funded by the U.S. Department of Energy (DOE), Office of Science, Basic Energy Sciences (BES). The development of the excited state electronic structure method is funded by National Science Foundation Grant CHE-1856210. The development of nuclear–electronic orbital time-dependent density functional theory methods is supported by National Science Foundation Grant CHE-1954348. Computations were facilitated through the use of advanced computational, storage, and networking infrastructure provided by the Hyak supercomputer system at the University of Washington, funded by the Student Technology Fee.

REFERENCES

- Hammes-Schiffer, S.; Soudackov, A. V. Proton-Coupled Electron Transfer in Solution, Proteins, and Electrochemistry. *J. Phys. Chem. B* **2008**, *112*, 14108–14123.
- Negele, J. W. The Mean-Field Theory of Nuclear Structure and Dynamics. *Rev. Mod. Phys.* **1982**, *54*, 913.
- Li, X.; Tully, J. C.; Schlegel, H. B.; Frisch, M. J. Ab Initio Ehrenfest Dynamics. *J. Chem. Phys.* **2005**, *123*, 084106.
- Tully, J. C.; Preston, R. K. Trajectory Surface Hopping Approach to Nonadiabatic Molecular Collisions: The Reaction of H⁺ with D₂. *J. Chem. Phys.* **1971**, *55*, 562.
- Subotnik, J. E.; Jain, A.; Landry, B.; Petit, A.; Ouyang, W.; Bellonzi, N. Understanding the Surface Hopping View of Electronic Transitions and Decoherence. *Annu. Rev. Phys. Chem.* **2016**, *67*, 387–417.
- Wang, L.; Akimov, A.; Prezhdo, O. V. Recent Progresses in Surface Hopping: 2011–2015. *J. Phys. Chem. Lett.* **2016**, *7*, 2100–2112.
- Ben-Nun, M.; Quenneville, J.; Martínez, T. J. Ab Initio Multiple Spawning: Photochemistry from First Principles Quantum Molecular Dynamics. *J. Phys. Chem. A* **2000**, *104*, 5161–5175.
- Mignolet, B.; Curchod, B. F. E. Excited-State Molecular Dynamics Triggered by Light Pulses–Ab Initio Multiple Spawning vs Trajectory Surface Hopping. *J. Phys. Chem. A* **2019**, *123*, 3582–3591.
- Beck, M. H.; Jäckle, A.; Worth, G. A.; Meyer, H.-D. The Multiconfiguration Time-Dependent Hartree (MCTDH) Method: A Highly Efficient Algorithm for Propagating Wavepackets. *Phys. Rep.* **2000**, *324*, 1–105.
- Wang, H.; Thoss, M. Multilayer Formulation of the Multiconfiguration Time-Dependent Hartree Theory. *J. Chem. Phys.* **2003**, *119*, 1289.
- Heller, E. J. Guided Gaussian Wave Packets. *Acc. Chem. Res.* **2006**, *39*, 127–134.
- Fischer, S. A.; Chapman, C. T.; Li, X. Surface Hopping with Ehrenfest Excited Potential. *J. Chem. Phys.* **2011**, *135*, 144102.
- Isborn, C. M.; Li, X.; Tully, J. C. TDDFT Ehrenfest Dynamics: Collisions between Atomic Oxygen and Graphite Clusters. *J. Chem. Phys.* **2007**, *126*, 134307.
- Ding, F.; Goings, J. J.; Liu, H.; Lingerfelt, D. B.; Li, X. Ab Initio Two-Component Ehrenfest Dynamics. *J. Chem. Phys.* **2015**, *143*, 114105.
- Goings, J. J.; Lingerfelt, D. B.; Li, X. Can Quantized Vibrational Effects Be Obtained from Ehrenfest Mixed Quantum-Classical Dynamics? *J. Phys. Chem. Lett.* **2016**, *7*, 5193–5197.
- Webb, S. P.; Iordanov, T.; Hammes-Schiffer, S. Multiconfigurational Nuclear-Electronic Orbital Approach: Incorporation of Nuclear Quantum Effects in Electronic Structure Calculations. *J. Chem. Phys.* **2002**, *117*, 4106.
- Yang, Y.; Brorsen, K. R.; Culpitt, T.; Pak, M. V.; Hammes-Schiffer, S. Development of a Practical Multicomponent Density Functional for Electron-Proton Correlation to Produce Accurate Proton Densities. *J. Chem. Phys.* **2017**, *147*, 114113.
- Zhao, L.; Tao, Z.; Pavošević, F.; Wildman, A.; Hammes-Schiffer, S.; Li, X. Real-Time Time-Dependent Nuclear-Electronic Orbital Approach: Dynamics Beyond the Born-Oppenheimer Approximation. *J. Phys. Chem. Lett.* **2020**, *11*, 4052–4058.
- Pavošević, F.; Tao, Z.; Culpitt, T.; Zhao, L.; Li, X.; Hammes-Schiffer, S. Frequency and Time Domain Nuclear-Electronic Orbital Equation-of-Motion Coupled Cluster Methods: Combination Bands and Electronic-Protonic Double Excitations. *J. Phys. Chem. Lett.* **2020**, *11*, 6435–6442.
- Pavošević, F.; Culpitt, T.; Hammes-Schiffer, S. Multicomponent Quantum Chemistry: Integrating Electronic and Nuclear Quantum Effects via the Nuclear-Electronic Orbital Method. *Chem. Rev.* **2020**, *120*, 4222–4253.
- Li, X.; Govind, N.; Isborn, C.; DePrince, A. E.; Lopata, K. Real-Time Time-Dependent Electronic Structure Theory. *Chem. Rev.* **2020**, *120*, 9951–9993.
- Zhao, L.; Wildman, A.; Pavošević, F.; Tully, J. C.; Hammes-Schiffer, S.; Li, X. Excited State Intramolecular Proton Transfer with Nuclear-Electronic Orbital Ehrenfest Dynamics. *J. Phys. Chem. Lett.* **2021**, *12*, 3497–3502.
- Tomasi, J.; Mennucci, B.; Cammi, R. Quantum Mechanical Continuum Solvation Models. *Chem. Rev.* **2005**, *105*, 2999–3094.
- Mennucci, B.; Cammi, R. *Continuum Solvation Models in Chemical Physics: From Theory to Applications*; John Wiley & Sons: 2008.
- Tomasi, J.; Persico, M. Molecular Interactions in Solution: An Overview of Methods Based on Continuous Distributions of the Solvent. *Chem. Rev.* **1994**, *94*, 2027–2094.
- Mennucci, B. Polarizable Continuum Model. *WIREs Comput. Mol. Sci.* **2012**, *2*, 386–404.
- Cances, E.; Mennucci, B.; Tomasi, J. A New Integral Equation Formalism for the Polarizable Continuum Model: Theoretical Background and Applications to Isotropic and Anisotropic Dielectrics. *J. Chem. Phys.* **1997**, *107*, 3032–3041.
- Liang, W.; Chapman, C. T.; Ding, F.; Li, X. Modeling Ultrafast Solvated Electronic Dynamics Using Time-dependent Density Functional Theory and Polarizable Continuum Model. *J. Phys. Chem. A* **2012**, *116*, 1884–1890.
- Nguyen, P.; Ding, F.; Fischer, S. A.; Liang, W.; Li, X. Solvated First-principles Excited State Charge Transfer Dynamics with Time-dependent Polarizable Continuum Model and Solvent Dielectric Relaxation. *J. Phys. Chem. Lett.* **2012**, *3*, 2898–2904.
- Corni, S.; Pipolo, S.; Cammi, R. Equation of Motion for the Solvent Polarization Apparent Charges in the Polarizable Continuum Model: Application to Real-Time TDDFT. *J. Phys. Chem. A* **2015**, *119*, 5405–5416.
- Ding, F.; Lingerfelt, D. B.; Mennucci, B.; Li, X. Time-dependent Non-equilibrium Dielectric Response in QM/Continuum Approaches. *J. Chem. Phys.* **2015**, *142*, 034120.

- (32) Chapman, C. T.; Liang, W.; Li, X. Solvent Effects on Intramolecular Charge Transfer Dynamics in a Fullerene Derivative. *J. Phys. Chem. A* **2013**, *117*, 2687–2691.
- (33) Marcus, R. A. On the Theory of Oxidation-Reduction Reactions Involving Electron Transfer. I. *J. Chem. Phys.* **1956**, *24*, 966–978.
- (34) Cammi, R.; Tomasi, J. Nonequilibrium Solvation Theory for the Polarizable Continuum Model: a New Formulation at the SCF Level with Application to the Case of the Frequency-Dependent Linear Electric Response Function. *Int. J. Quantum Chem.* **1995**, *56*, 465–474.
- (35) Mennucci, B.; Cammi, R.; Tomasi, J. Excited States and Solvatochromic Shifts within a Nonequilibrium Solvation Approach: A New Formulation of the Integral Equation Formalism Method at the Self-Consistent Field, Configuration Interaction, and Multi-configuration Self-Consistent Field Level. *J. Chem. Phys.* **1998**, *109*, 2798–2807.
- (36) Krumland, J.; Gil, G.; Corni, S.; Cocchi, C. LayerPCM: An Implicit Scheme for Dielectric Screening from Layered Substrates. *J. Chem. Phys.* **2021**, *154*, 224114.
- (37) Caricato, M.; Ingrosso, F.; Mennucci, B.; Tomasi, J. A Time-Dependent Polarizable Continuum Model: Theory and Application. *J. Chem. Phys.* **2005**, *122*, 154501.
- (38) Li, X.; Williams-Young, D.; Valeev, E. F.; Petrone, A.; Sun, S.; Stetina, T.; Kasper, J. *Chronus Quantum*, ver. Beta 2; 2018. <http://www.chronusquantum.org>.
- (39) Williams-Young, D. B.; Petrone, A.; Sun, S.; Stetina, T. F.; Lestranger, P.; Hoyer, C. E.; Nascimento, D. R.; Koulias, L.; Wildman, A.; Kasper, J.; et al. The Chronus Quantum Software Package. *WIREs Comput. Mol. Sci.* **2020**, *10*, e1436.
- (40) Dunning, T. H. Gaussian Basis Sets for Use in Correlated Molecular Calculations. I. The Atoms Boron through Neon and Hydrogen. *J. Chem. Phys.* **1989**, *90*, 1007.
- (41) Yu, Q.; Pavošević, F.; Hammes-Schiffer, S. Development of Nuclear Basis Sets for Multicomponent Quantum Chemistry Methods. *J. Chem. Phys.* **2020**, *152*, 244123.
- (42) Stephens, P. J.; Devlin, F. J.; Chabalowski, C. F.; Frisch, M. J. Ab Initio Calculation of Vibrational Absorption and Circular Dichroism Spectra Using Density Functional Force Fields. *J. Phys. Chem.* **1994**, *98*, 11623–11627.
- (43) Becke, A. Density-Functional Thermochemistry. III. The Role of Exact Exchange. *J. Chem. Phys.* **1993**, *98*, 5648.
- (44) Lee, C.; Yang, W.; Parr, R. G. Development of the Colle-Salvetti Correlation-Energy Formula into a Functional of the Electron Density. *Phys. Rev. B* **1988**, *37*, 785–789.
- (45) Vosko, S. H.; Wilk, L.; Nusair, M. Accurate Spin-Dependent Electron Liquid Correlation Energies for Local Spin Density Calculations: a Critical Analysis. *Can. J. Phys.* **1980**, *58*, 1200–1211.
- (46) Brorsen, K. R.; Yang, Y.; Hammes-Schiffer, S. Multicomponent Density Functional Theory: Impact of Nuclear Quantum Effects on Proton Affinities and Geometries. *J. Phys. Chem. Lett.* **2017**, *8*, 3488–3493.
- (47) Di Remigio, R.; Frediani, L.; et al. *PCMSolver*. <http://pcmsolver.readthedocs.io/>.
- (48) Bondi, A. v. van der Waals Volumes and Radii. *J. Phys. Chem.* **1964**, *68*, 441–451.
- (49) Gerardi, H. K.; DeBlase, A. F.; Su, X.; Jordan, K. D.; McCoy, A. B.; Johnson, M. A. Unraveling the Anomalous Solvatochromic Response of the Formate Ion Vibrational Spectrum: An Infrared, Ar-Tagging Study of the HCO₂, DCO₂, and HCO₂⁻·H₂O ions. *J. Phys. Chem. Lett.* **2011**, *2*, 2437–2441.
- (50) Dunning, T. H., Jr Gaussian Basis Sets for Use in Correlated Molecular Calculations. I. The Atoms Boron through Neon and Hydrogen. *J. Chem. Phys.* **1989**, *90*, 1007–1023.
- (51) Wilson, A. K.; van Mourik, T.; Dunning, T. H., Jr. Gaussian Basis Sets for Use in Correlated Molecular Calculations. VI. Sextuple Zeta Correlation Consistent Basis Sets for Boron through Neon. *J. Mol. Struct.: THEOCHEM* **1996**, *388*, 339–349.
- (52) Barone, V. Anharmonic Vibrational Properties by a Fully Automated Second-Order Perturbative Approach. *J. Chem. Phys.* **2005**, *122*, 014108.
- (53) Frisch, M. J.; Trucks, G. W.; Schlegel, H. B.; Scuseria, G. E.; Robb, M. A.; Cheeseman, J. R.; Scalmani, G.; Barone, V.; Petersson, G. A.; Nakatsuji, H.; et al. *Gaussian 16*, rev. A.03; Gaussian Inc.: Wallingford, CT, 2016.
- (54) Forney, D.; Jacox, M. E.; Thompson, W. E. Infrared Spectra of trans-HOCO, HCOOH⁺, and HCO₂⁻ Trapped in Solid Neon. *J. Chem. Phys.* **2003**, *119*, 10814–10823.
- (55) Ito, K.; Bernstein, H. J. The Vibrational Spectra of the Formate, Acetate, and Oxalate Ions. *Can. J. Chem.* **1956**, *34*, 170–178.
- (56) Błasiak, B.; Londergan, C. H.; Webb, L. J.; Cho, M. Vibrational Probes: From Small Molecule Solvatochromism Theory and Experiments to Applications in Complex Systems. *Acc. Chem. Res.* **2017**, *50*, 968–976.
- (57) Donati, G.; Wildman, A.; Caprasecca, S.; Lingerfelt, D. B.; Lipparini, F.; Mennucci, B.; Li, X. Coupling Real-time Time-dependent Density Functional Theory with Polarizable Force Field. *J. Phys. Chem. Lett.* **2017**, *8*, 5283–5289.
- (58) Zhao, L.; Wildman, A.; Tao, Z.; Schneider, P.; Hammes-Schiffer, S.; Li, X. Nuclear-Electronic Orbital Ehrenfest Dynamics. *J. Chem. Phys.* **2020**, *153*, 224111.
- (59) Yang, Y.; Schneider, P. E.; Culpitt, T.; Pavošević, F.; Hammes-Schiffer, S. Molecular Vibrational Frequencies within the Nuclear-Electronic Orbital Framework. *J. Phys. Chem. Lett.* **2019**, *10*, 1167–1172.
- (60) Formosinho, S. J.; Arnaut, L. G. Excited-State Proton Transfer Reactions II. Intramolecular Reactions. *J. Photochem. Photobiol., A* **1993**, *75*, 21–48.
- (61) Aquino, A. J. A.; Lischka, H.; Hättig, C. Excited-State Intramolecular Proton Transfer: A Survey of TDDFT and RI-CC2 Excited-State Potential Energy Surfaces. *J. Phys. Chem. A* **2005**, *109*, 3201–3208.